European Journal of Medicinal Chemistry 46 (2011) 2937–2947

Contents lists available at ScienceDirect

European Journal of Medicinal Chemistry

journal homepage: http://www.elsevier.com/locate/ejmech

Original article

Pharmacophore based virtual screening, molecular docking studies to design potent heat shock protein 90 inhibitors

Sugunadevi Sakkiah, Sundarapandian Thangapandian [1], Shalini John [1], Keun Woo Lee*

Division of Applied Life Science (BK21 Program), Plant Molecular Biology and Biotechnology Research Center (PMBBRC), Department of Chemistry and Research Institute, Gyeongsang National University (GNU), 900 Gazwa-dong, Jinju 660-701, Republic of Korea

ARTICLE INFO

Article history:
Received 7 February 2011
Received in revised form
30 March 2011
Accepted 4 April 2011
Available online 15 April 2011

Keywords:
Heat shock protein 90
Common feature hypothesis
Structure-based pharmacophore
LigandScout
Virtual screening
GOLD

ABSTRACT

The identification of important chemical features of Heat Shock Protein 90 (HSP90) inhibitors will be helpful to discover the potent candidate to inhibit the HSP90 activity. The best hypothesis from Hip-Hop, Hypo1, one hydrogen bond donor (HBD), two hydrogen bond acceptors (HBA), and two hydrophobic (H) and structure-based hypothesis, SB_Hypo1, one HBA, one HBD and four H features, were generated using Discovery Studio and LigandScout, respectively. Test and decoy sets were used to corroborate the best hypotheses and the validated hypotheses were used to screen the chemical databases. Subsequently, the screened compounds were filtered by applying the rule of five, ADMET and molecular docking. Finally, four compounds were obtained as novel leads to inhibit the HSP90 activity.

1. Introduction

Molecular chaperones, mainly responsible for protein folding and its 3D conformation in the cell, also plays a crucial roles in balancing the degradation and synthesis of many proteins [1]. Among many chaperones, Heat Shock Protein (HSP) is the most important because it protects the cells when stressed elevated by temperature [2]. The 90-kDa Heat Shock Protein (HSP90), an ATP-dependent molecular chaperon, is one of the vital targets in chemogenomic approaches [3] as well as highly conserved from bacteria to human [4–6]. Human HSP90 family includes 17 genes which were classified into 4 classes: HSP90AA, HSP90AB, HSP90B, and TRAP [7]. HSP90 plays a major role in folding and maturation of various client proteins such as steroid receptors, p53, ErbB2, Src, Abl, Raf, Akt and cyclin-dependent serine kinases [2]. HSP90 consists of three distinct domains [8]: N-terminal, middle and C-terminal domains. The N- and C- terminal domains are mainly focused in many pharmaceutical companies to design the new inhibitors. N-terminal, ATP binding domain interacts with many synthetic inhibitors as well as the natural products and the C-terminal domain plays an important role in homo-dimerisation process [9]. Inhibition of HSP90 leads to deregulation of many crucial pathways such as (a) self-sufficiency in growth signals (b) tissues invasion/metastasis (c) insensitivity to antigrowth signals (d) sustained angiogenesis (e) evasion of apoptosis and (f) limitless replicative potential which are responsible for the cancer cell's survival [10] as well as it involves in the destabilization and degradation of oncogenic client proteins to stop the cancer cell growth [5]. Blocking the ATPase activity of HSP90 will be an important pharmacological platform in anticancer therapy [11]. The majorities of inhibitors developed so far inhibit the HSP90 by binding in ATP-binding pocket which drives the chaperon's cycle and direct interactions induce the active conformation [12]. Geldanamycin and its derivatives are the natural products to inhibit the ATPase activity by binding in the N-terminal domain of HSP90 [13] and reported as a potent cancer drugs. Hence, the N-terminal domain is a substantial target in structure biology approaches that facilitate the structure-based inhibitor optimization [14]. Inhibitors of HSP90 are classified into several classes based on distinct modes of inhibition like (a) blockade of ATP binding, (b) disruption of co-chaperon/HSP90 interactions, (c) antagonism of client/HSP90 associations and (d) interference with post-translational modifications of HSP90 [15]. All the above inhibition makes HSP90 as a potential target for many diseases ranging from the disruption of multiple signaling pathways associated with cancer [16,17] and also in the clearance of protein aggregates in neurodegenerative diseases [18]. Thus, discovery of small molecule inhibitors of HSP90 remains an active field of cancer research [19].

* Corresponding author. Tel.: +82 55 751 6276; fax: +82 55 752 7062.
E-mail address: kwlee@gnu.ac.kr (K.W. Lee).
[1] Contributed equally as second author.

0223-5234/$ – see front matter © 2011 Elsevier Masson SAS. All rights reserved.
doi:10.1016/j.ejmech.2011.04.018

The computational techniques help in drug design process to dramatically widen the chemical space and reduce the number of candidates for experimental validation [20]. Pharmacophore modeling and virtual screening is an inexpensive and fast alternative powerful tool to identify the potential lead for various targets [17,21]. Hence in this study, ligand and structure-based pharmacophore models were generated and validated using the test and decoy sets. In a wide variety of applications, virtual screening was found to be successful method especially when combined with molecular docking studies. Hence the predicted hypotheses have been employed in virtual screening to identify the potent lead from various databases such as Maybridge [22] and Chembridge [23]. The retrieved hit molecules are sorted out by applying several filters such as maximum fit value of the best pharmacophore models from ligand-based, structure-based hypotheses and satisfy the Lipinski's Rule of five, ADME properties and subsequently subjected to molecular docking process. The molecular docking studies were performed using two different programs, *LigandFit*/Discovery Studio v2.5 (DS, Accelrys) [24] and *Genetic Optimization for Ligand Docking* (GOLD, Cambridge Crystallographic Data Center) [25] to find the suitable orientation of leads in the active site of HSP90.

2. Results and discussions

2.1. Ligand based pharmacophore modeling using DS

The qualitative top ten hypotheses were generated based on the training set molecules (Fig. 1) using *Common Feature Pharmacophore Generation*/DS to identify the common features necessary to inhibit the HSP90 function. Direct and partial hit mask value of '1' and '0' for hypothesis indicated that the molecules present in dataset are well mapped to all the chemical features in the hypothesis and there is no partial mapping or missing features specified in Table 1. The *Cluster analysis* (Fig. 2) was used to evaluate and categorized the difference between the compositions of hypothesis chemical features and locations. This process gives the number of clusters, in this paper two clusters are selected based on the features similarities. Cluster I contains six hypotheses with the combination of three chemical features like hydrogen bond acceptor (HBA), hydrogen bond donor (HBD) and hydrophobic (H) and Cluster II contains four hypotheses that contains two chemical features (HBA and H). Focusing on above the two Clusters there was only one chemical feature (HBA or HBD) was different from Cluster I and II. Hence, initially one pharmacophore model was selected as a good hypothesis from each cluster with high ranking score: Cluster I-Hypo1: two HBA, two HBD, one H and Cluster II-Hypo2: two HBA and three H. Among these two hypotheses, Hypo1 has the highest ranking score (54.562) when compared with Hypo2 (53.562). Hence Hypo1 was selected as a best qualitative pharmacophore models based on the chemical features similarities, ranking score and their corresponding geometric constrains. Hypo1 shows the good alignment with the training set molecules has shown in Fig. 3.

Table 1
Details of the top ten hypotheses generated using Hip-Hop for HSP90.

Hypothesis Name	Features[a]	Rank[b]	Direct hit[c]	Partial hit[c]	Max. fit
Hypo1	H, H, HBD, HBA, HBA	54.56	11111	00000	5
Hypo2	H, H, HBA, HBA, HBA	53.56	11111	00000	5
Hypo3	H, H, HBD, HBA, HBA	53.30	11111	00000	5
Hypo4	H, H, HBD, HBA, HBA	52.13	11111	00000	5
Hypo5	H, H, HBA, HBA, HBA	52.30	11111	00000	5
Hypo6	H, H, HBA, HBA, HBA	52.13	11111	00000	5
Hypo7	H, H, HBD, HBA, HBA	52.03	11111	00000	5
Hypo8	H, H, HBD, HBA, HBA	51.90	11111	00000	5
Hypo9	H, H, HBD, HBA, HBA	51.54	11111	00000	5
Hypo10	H, H, HBA, HBA, HBA	51.03	11111	00000	5

[a] HBA = Hydrogen Bond Acceptor; HBD = Hydrogen Bond Donor; H = Hydrophobic.
[b] Higher the ranking score, lesser the probability of chance correlation. The best hypothesis shows the highest value.
[c] Direct Hit, Partial Hit indicates whether (1) or (0) a training set molecule mapped every feature of the hypothesis and mapped to all but one feature in the hypothesis. The numbers from (right to left) correspond to the compounds (from top to bottom).

2.2. Structure-based pharmacophore modeling

The 40 co-crystal structures from Protein Data Bank (PDB, www.rcsb.org) has been checked for a better understanding of the specificity and pharmacophore requirements of HSP90 active site (Table 2). The binding site was characterized by several direct

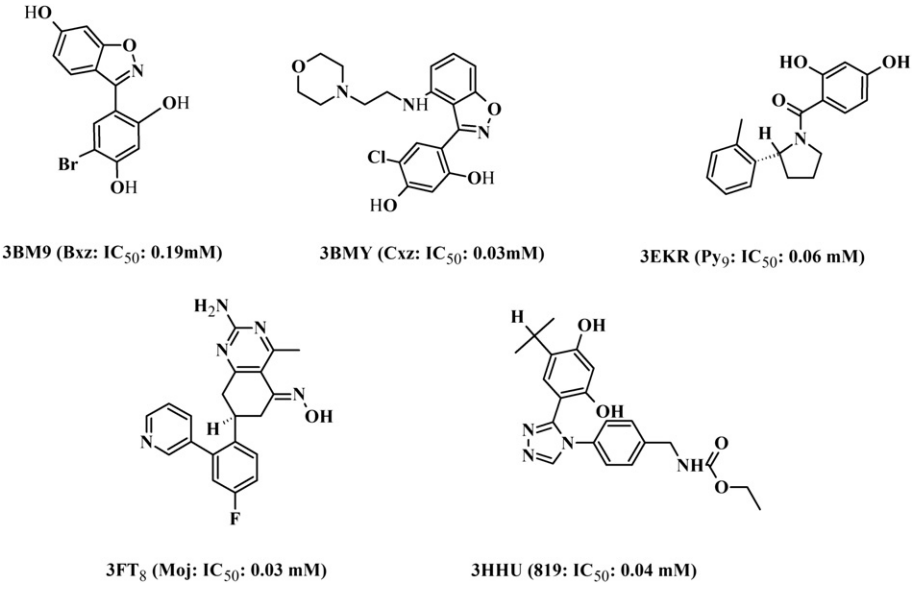

Fig. 1. Structure of five compounds used as training set in Hip-Hop, PDB ID, IC_{50} values and their corresponding co-crystal name was given in bracket.

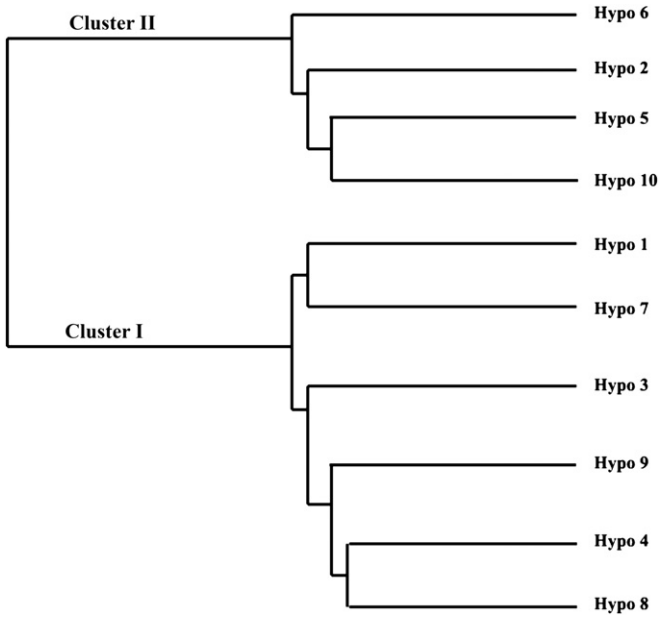

Fig. 2. Phylogenic Cluster analysis for ligand-based common feature hypothesis.

interactions such as hydrogen bond interaction and liphophilic side chains complement which reflect the hydrophobic nature of the HSP90 active site. The active site of the five co-crystal structures were visualized and analyzed for protein–ligand interactions (Fig. 4) [26] which was the most important starting point for the generation of structure-based pharmacophore.

2.2.1. Generation of structure-based pharmacophore models using LigandScout

LigandScout present the interactions between protein and ligand as well as with some excluded volume spheres corresponding to their 3D structures of protein. In this study, five different 3D structure of HSP90 bound with its inhibitors such as 3BM9 [27], 3BMY [28], 3FT8 [27], 3HHU [29], 3EKR [30] were selected as input for structure-based pharmacophore generation. The generated five pharmacophore models with its geometrical constrain and their active sites were represented in Fig. 5. For 3BM9 complex, the generated pharmacophore contains two HBA pointed towards the Lys58, Thr184, one HBD chemical feature which pointed towards Asp93, two H groups and 12 excluded volume spheres. Four features

Table 2
Analyses of critical amino acids for HSP90 inhibition from 40 co-crystal structures deposited in protein data bank.

PDB ID	Asn51	Asp93	Lys58	Asp93	Gly97	Phe138	Gly97	Thr184
3BM9[27]			√	√	√	√	√	√
3BMY[27]	√	√		√		√	√	√
3EKR [30]	√	√		√	√		√	√
2BYI [41]	√	√	√	√	√	√	√	√
2BYH[41]	√	√		√	√	√	√	√
2VCJ [42]	√	√		√	√		√	√
2VCI [42]	√	√	√	√	√	√	√	√
3D0B [43]		√		√	√			√
1YC3 [44]	√	√	√	√	√	√	√	√
1YET [45]	√	√	√	√		√		√
2QG0 [46]	√	√	√	√	√		√	√
2QFO [46]	√	√		√	√		√	√
2QG2 [46]	√			√		√	√	√
2QF6 [46]		√		√	√	√		√
1OSF [47]	√	√	√	√		√		√
2CDD[48]	√	√	√	√	√	√	√	√
2CCS [49]	√	√		√	√	√	√	√
2CCU[49]		√		√	√		√	√
2CCT [49]	√		√	√	√	√	√	√
1UY6 [50]	√	√		√	√	√		√
1UY7 [50]	√	√		√	√			√
1UYM[50]		√		√		√		√
1UYI [50]	√	√		√	√	√	√	√
1UYK[50]	√	√		√	√		√	√
1UYH[50]	√	√		√	√	√	√	√
1UYG[50]	√	√		√	√	√	√	√
1UYF [50]	√	√		√	√	√	√	√
1UYE [50]		√		√	√	√		√
1UY9 [50]		√		√	√	√		√
1UYC[50]	√	√		√	√	√		√
1UY8 [50]		√		√	√	√		√
1UYD[50]		√		√	√	√		√
2UWD[51]		√		√		√	√	√
2BSM[52]	√	√	√	√	√	√	√	√
2BT0 [52]	√	√		√		√	√	√
2FWY[53]	√	√		√	√	√		√
2H55 [53]	√	√		√	√	√	√	√
2FWZ [53]	√	√		√	√	√		√
2JJC[54]		√		√	√			√
2BZ5[14]	√	√	√	√	√	√	√	√
3EKO[55]	√	√	√	√	√			√

hypothesis was generated from 3BMY complex which composed of one HBA, one HBD, and two H groups with 10 excluded volume spheres. The HBD and HBA groups pointed towards the Asp93 and Thr184, respectively. 3FT8 complexes consists of six features hypothesis includes one HBA which pointed towards Thr184, one

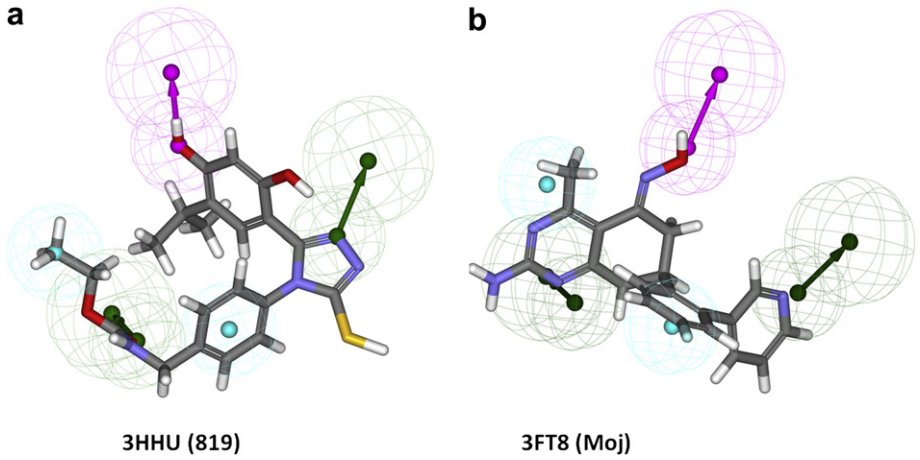

Fig. 3. Training set compounds shown good alignment with Hypo1. Green color indicates hydrogen bond acceptor (HBA); cyan indicates hydrophobic (H) and magenta indicates hydrogen bond donor (HBD) (for interpretation of the references to colour in this figure legend, the reader is referred to the web version of this article.)

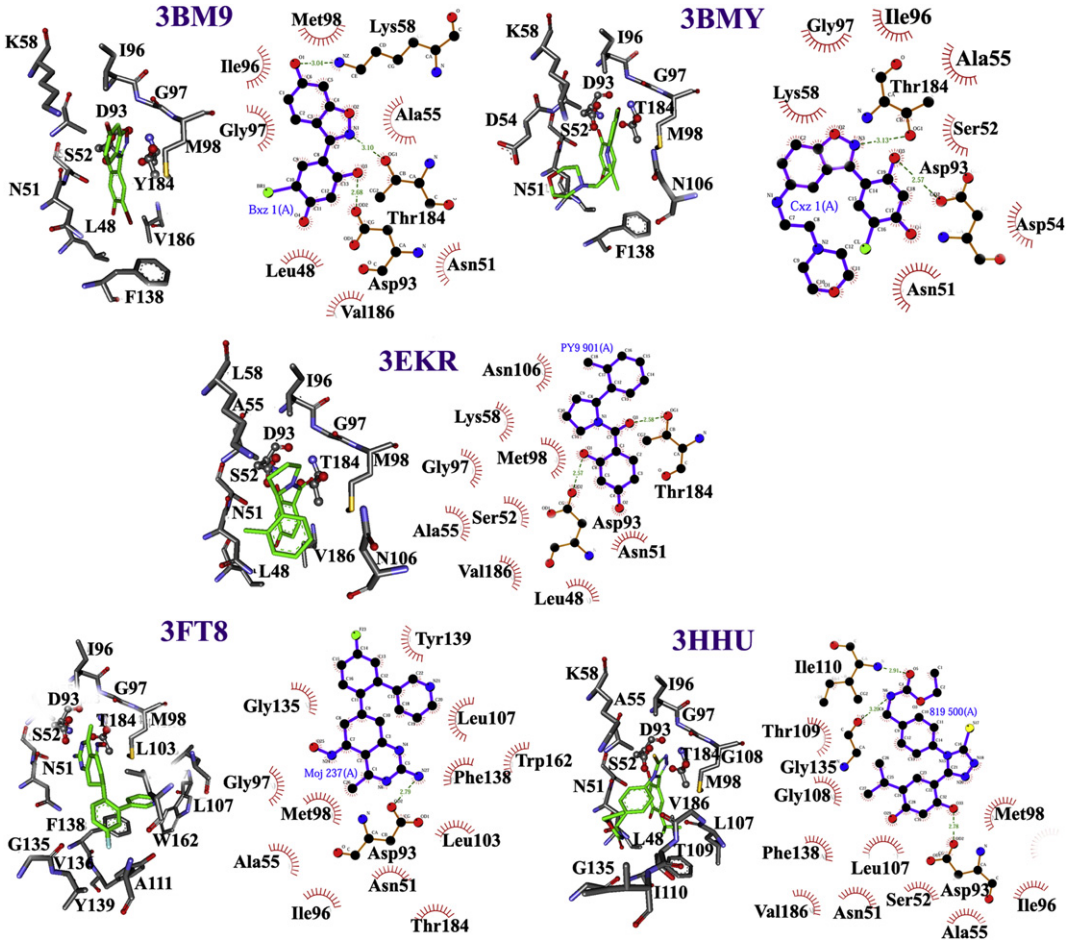

Fig. 4. Active site of five crystal structures of HSP90 bound with its inhibitors.

HBD pointed towards Asp93, and four H groups with 16 excluded volume spheres. Six features hypothesis was generated from 3HHU complex that includes two HBA, one HBD, and three H groups with 14 excluded volume spheres. The two HBA groups pointed towards the Ile110, Gly135 and HBD pointed towards Asp92. 3EKR complex produced seven features hypothesis consists of two HBA, one HBD, and four H groups with 11 excluded volume spheres. The two HBA and HBD groups pointed towards the Thr184, Asn51 and Asp93, respectively.

Comparing the above five pharmacophore models, one HBD and HBA from all the models were pointed towards Asp93 and Thr184 which plays a major role in HSP90 activity, respectively. Hence, HBD and HBA features are considered as important chemical features to discover the novel HSP90 inhibitors. The dynamic structure-based pharmacophore was generated by superimposing the five structure-based hypothesis and the overlapped chemical features were removed. Finally eight features dynamics structure-based hypothesis (Fig. 6) was produced that consists of 3 HBA, 1 HBD and 4 H features. Due to the high number of chemical features the dynamics structure-based model (8 features hypothesis) has been split into two different hypothesis which contain six features each, SB_Hypo1 and SB_Hypo2 contain one HBA, one HBD, four H features and three HBA, one HBD, two H groups, respectively (Fig. 7).

2.3. Validation of ligand and structure-based pharmacophore models

The best hypothesis from Hip-Hop (Hypo1) and dynamics structure-based models (SB_Hypo1 and SB_Hypo2) were validated using two different methods: (i) test set, to validate how well our selected hypothesis pick the active from inactive compounds (ii) decoy set, to evaluate the predictability of the selected hypothesis using statistical parameters. The test set contains 30 structurally diverse molecules that was classified into three different categories based on its IC_{50} values (explained in Methods and materials), i.e., highly active, moderately active and low active compounds. The qualitative hypothesis (Hypo1) and dynamics structure-based hypothesis (SB_Hypo1) are screened all the molecules present in the test set but it produces a high fit value for the active and moderately active compounds when compared with the low active compounds. In case of dynamics structure-based hypothesis, SB_Hypo2, select few active and moderate compounds but fails to choose the low active compounds as well as some of the active compounds (Table 3). Comparing the structure-based hypothesis, the hit compounds from SB_Hypo1 comprises all compounds screened by SB_Hypo2 hypothesis. Hence, SB_Hypo1 was selected as a best structure-based pharmacophore model for the HSP90 receptor.

2.4. Enrichment of database

In drug discovery process, the best hypothesis should identify the active compounds from inactive. Decoy set, comprises of 25 known good inhibitors and 1975 decoy molecules of HSP90 inhibitors, was used to validate whether the hypotheses (Hypo1, SB_Hypo1) could able to discriminate the active from inactive compounds or not. The database screening was performed using

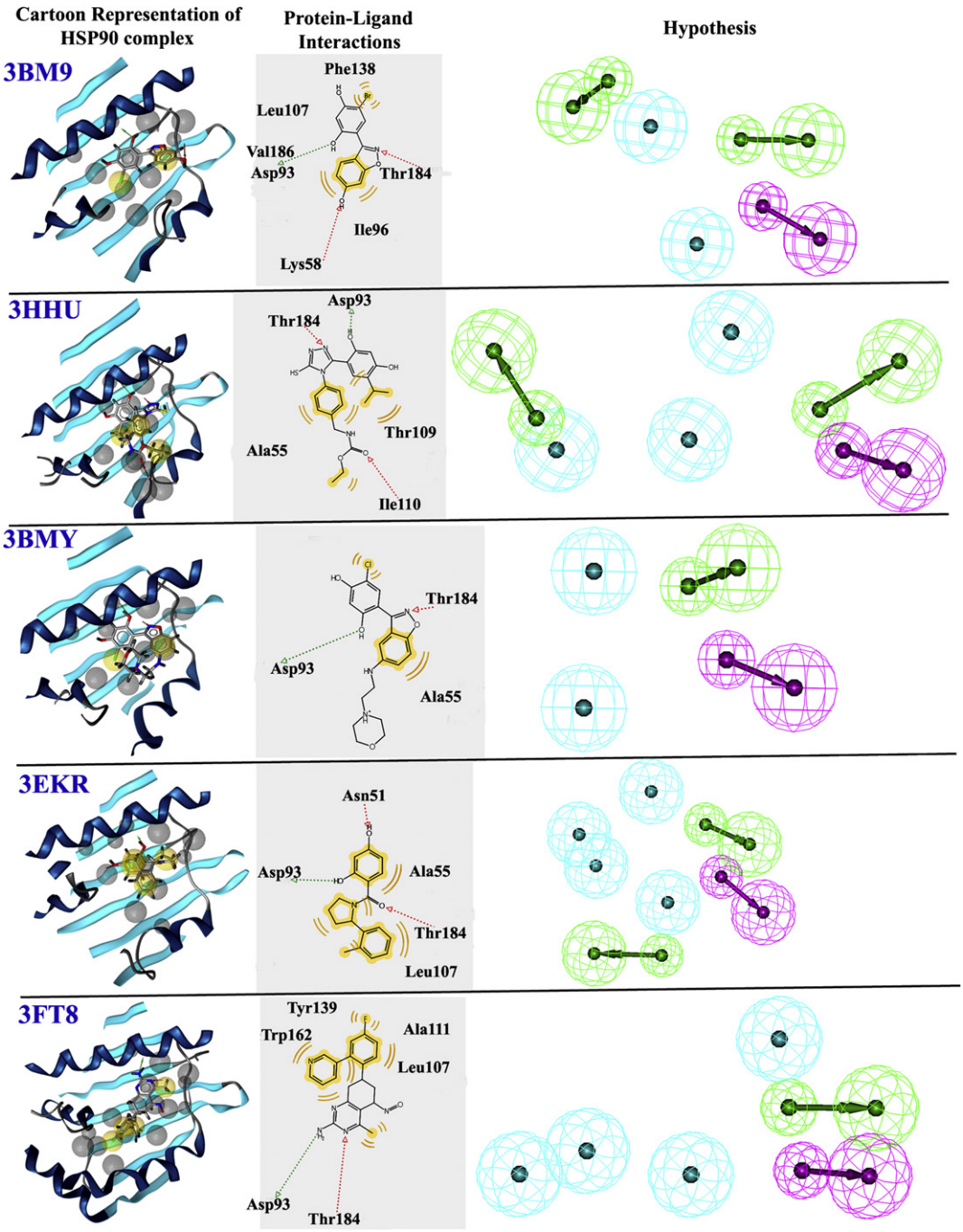

Fig. 5. Structure-based hypotheses were superimposed on the active site of 3D structure of HSP90. Green color indicates hydrogen bond acceptor (HBA); cyan indicates hydrophobic (H) and magenta indicates hydrogen bond donor (HBD). Red arrow represents the hydrogen bond acceptor (HBA); Green arrow represents the hydrogen bond donor (HBD); Brown color indicates hydrophobic (H) (for interpretation of the references to colour in this figure legend, the reader is referred to the web version of this article.)

Ligand Pharmacophore Mapping module. The result was analyzed using a set of parameters such as hit list (H_t), number of active percent of yields (%Y), percent ratio of actives in the hit list (%A), enrichment factor (E), false negatives, false positives, and goodness of hit score (GH) (Table 4) [31]. Hypo1 and SB_Hypo1 were successfully retrieved 100% and 88% of active compounds from the decoy set, respectively. In addition Hypo1 and SB_Hypo1 have shown an enrichment factor of 4.1 and 3.2 as well as the GH score of 0.89 and 0.71, respectively, which indicates that the quality of the pharmacophore models are acceptable. By overall validations, we can assure that both the hypotheses were able to predict most of the compounds in the same order of magnitude and it can able to discriminate the active inhibitors form inactive or low active compounds. Hence, we suggested that Hypo1 and SB_Hypo1 hypotheses are good to select or discriminated the suitable inhibitors of HSP90.

2.5. Database screening

From the above validation methods, it was proved that Hypo1 and SB_Hypo1 have superior ability to distinguish the active and inactive inhibitors of HSP90. The representative pharmacophore,

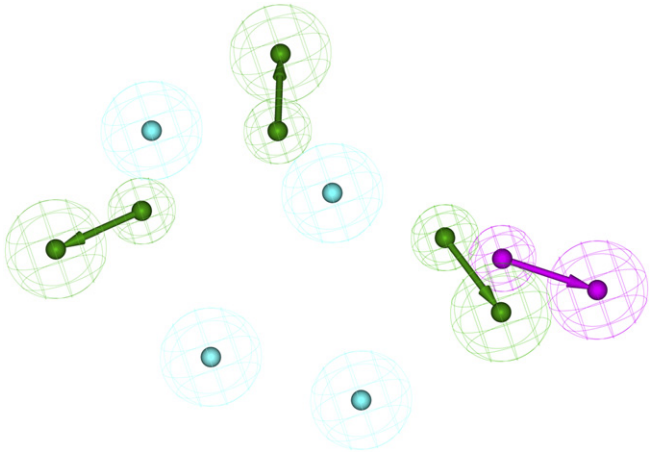

Fig. 6. Eight feature hypothesis after removal of overlapped chemical features from structure-based models. Green color indicates hydrogen bond acceptor (HBA); cyan indicates hydrophobic (H) and magenta indicates hydrogen bond donor (HBD). Red arrow represents the hydrogen bond acceptor (HBA); Green arrow represents the hydrogen bond donor (HBD); Brown color indicates hydrophobic (H) (for interpretation of the references to colour in this figure legend, the reader is referred to the web version of this article.)

Hypo1 and SB_Hypo1, have used as a 3D queries to screen the chemical databases like Maybridge and Chembridge consists of 60,000 and 50,000 compounds respectively. The initial screening of Hypo1 retrieved 16,236 from Maybridge, 12,923 from Chembridge and the retrieved hits were narrow down to 1100 and 543 compounds by applying the maximum fit value of 4, respectively. In case of SB_Hypo1, 15,187 and 12,814 compounds were selected and sorted out by applying a cut off value more than 4 (maximum fit value) 635 from Maybridge and 216 molecules from Chembridge, respectively. Moreover, ADME and Lipinski's rule of five were used to eliminate the non-drug like compounds from the hit molecules from Maybridge and Chembridge corresponded to 166, 166 and 36, 55, from Hypo1 and SB_Hypo1, respectively. Totally, 17 compounds were selected from Maybridge and Chembridge which satisfied all the chemical features present in Hypo1 and 19 compounds was sorted out from Maybridge and Chembridge using SB_Hypo1. These 17 and 19 compounds were used for further analysis like molecular docking studies to avoid the false positive hits from the virtual

Table 3
Fit values of each compounds in the test set using Hypo1, SB_Hypo1 and SB_Hypo2.

Compound No.	Exp.IC_{50} nM[a]	Fit Value		
		Hypo1	SB_Hypo1	SB_Hypo2
1	6	4.453	4.916	2.759
2	6	4.432	4.285	3.434
3	11	3.893	4.352	2.94
4	13	3.740	4.379	3.642
5	14	4.169	4.076	1.764
6	14	3.446	3.952	2.506
7	26	3.755	3.011	2.169
8	30	3.361	3.839	–
9	36	3.676	3.333	1.888
10	40	3.93	3.002	–
11	64	3.784	3.151	3.698
12	115	3.446	2.853	3.865
13	142	3.238	3.093	3.608
14	146	3.472	3.087	3.643
15	231	3.613	3.157	3.442
16	239	3.672	3.125	3.502
17	280	3.622	3.248	0.768
18	343	3.327	2.646	3.302
19	600	3.512	2.515	–
20	728	3.127	2.269	2.857
21	914	2.944	2.496	3.727
22	1000	2.548	2.935	2.522
23	1290	2.983	2.567	3.577
24	2630	2.708	2.742	3.785
25	4400	0.961	0.988	–
26	4730	1.239	2.619	–
27	6900	0.81	1.835	–
28	12800	0.567	3.046	–
29	75000	1.952	1.852	–
30	200000	0.078	0.358	–

[a] Activity scale: $IC_{50} < 300$ nM (highly active), 300 nM $\leq IC_{50} < 3000$ nM (moderately active), $IC_{50} \geq 3000$ nM (low active).

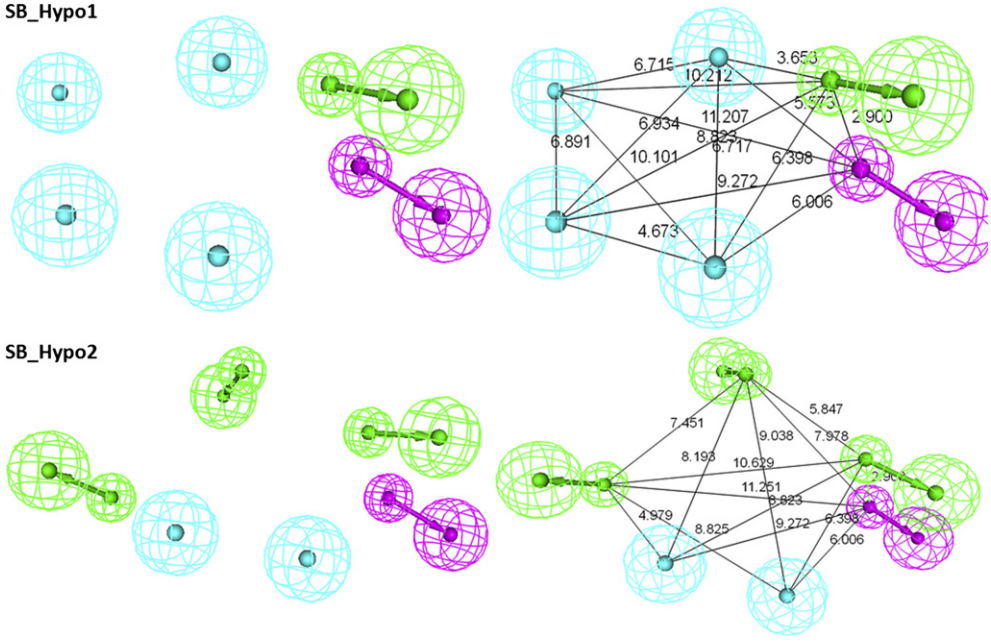

Fig. 7. Six features hypothesis: SB_Hypo1 and SB_Hypo2 and its geometric constrains. Green color indicates hydrogen bond acceptor (HBA); cyan indicates hydrophobic (H) and magenta indicates hydrogen bond donor (HBD) (for interpretation of the references to colour in this figure legend, the reader is referred to the web version of this article.)

Table 4
Statistical parameter from screening Decoy set.

No.	Parameter	Hypo1	SB_Hypo1
1	Total number of molecules in database (D)	1200	1200
2	Total number of actives in database (A)	25	25
3	Total number of hit molecules from the database (Ht)	29	33
4	Total number of active molecules in hit list (Ha)	25	22
5	% Yield of actives [(Ha/Ht) × 100]	86.21	66.66
6	% Ratio of actives [(Ha/A) × 100]	100	88
7	Enrichment Factor (EF)	4.1	3.2
8	False negatives [A-Ha]	0	3
9	False Positives [Ht − Ha]	4	11
10	Goodness of fit score [a] (GF)	0.89	0.71

[a] [(Ha/4HtA)(3A + Ht) x (1- ((Ht − Ha)/(D-A))]

screening process. The final leads which satisfied all the critical chemical features of Hypo1 and SB_Hypo1 as well as the ADME and Drug likeness properties are tabulated in Table 5.

2.6. Molecular docking studies

Molecular docking provides a visualization of potential binding orientations that display clearly the hydrogen bonding interactions with critical residues such as Thr184 and Asp93.

2.6.1. LigandFit/DS

Molecular docking is a computational technique that sample conformations of small compound in protein binding site; scoring functions are used to assess which of these conformations were best complements to the protein binding site. Molecular docking programs consists of two essential parts: an algorithm that searches the conformational, rotational and translational space available to candidate molecules within binding site and an objective function to be minimized during the process. All the selected hit compounds (36) and test set molecules (30) were docked into the active site of HSP90 to confirm the suitable binding orientation of the ligands and also to ensure its geometric fit within the active site. Flexible docking followed by consensus scoring method was performed to identify a suitable orientation of ligands in the active site of HSP90. LigScore1, LigScore2, Piecewise Linear Potential 1 (PLP1), Piecewise Linear Potential 2 (PLP2), Potential of mean force (PMF), Jain, Ludi and Dock score were used for the detection of HSP90 inhibitors. PLP scores were calculated based on the descriptions of hydrogen bonds forming. PMF scores were calculated by the summing pair-wise interaction terms over all inter-atomic pairs of the receptor–ligand complex. Dock score was considered as the degree of difficulty about ligand moving into the binding site. Jain and Ludi scores were consulted in hydrophobic interaction and degree of freedom, respectively. Before analyzing the docking result of the hit molecules, docking procedure was validated using the test set molecules. In the interpretation of docked test set molecules Jain scoring function was able to retrieve reasonable pose of the active molecules. Most of the sorted molecules, using Jain score, show good interactions with the critical residues like Asp93 and Try184. Hence the same analysis procedure has been performed for the hit molecules derived from a virtual screening process which picked out 8 and 7 molecules from Maybridge and Chembridge, respectively. To sort out these molecules visual inspection of the docked hit compounds were carried out to find the critical interactions of the small molecules with receptor. The main aim of this visualization process is to eliminate the molecules which are not able to show the hydrogen bond interactions with the critical residues present in the HSP90 active site. Based on the above analyzes, 3 and 1 from Maybridge and Chembridge databases were selected as a potent inhibitors of the HSP90.

2.6.2. GOLD analysis

GOLD docking was performed to find the interactions between the ATP binding site of HSP90 and ligands. The databases hit compounds (36) as well as the test set molecules (30) were used as input for GOLD docking, for each molecule 10 poses were saved and the corresponding gold fitness score were generated. Larger the fitness score of the ligand pose was better because it was calculated based on the negative of the sum of the component energy terms. The fitness function was optimized for the prediction of ligand binding position. The well orientated ligand pose has lowest energy with average Gold fitness score [32] were enumerated. In the case of test set molecules, most of the active compounds show an average fitness scores more than 25 and the inactive compounds have the average fitness score less than 25. From this analyzes it was confirmed that the active molecules of HSP90 shows the good fitness score. So, the above pre-validated analysis was used to sort

Table 5
ADME values for the selected compounds from Maybridge and Chembridge databases which satisfied all the chemical features of Hypo1 and SB_Hypo1.

Maybridge			Chembridge		
Name	Brain Blood Barrier (BBB)	Solubility	Name	Brain Blood Barrier (BBB)	Solubility
BTB03651	−0.876	−3.057	Compound10905	−1.185	−2.717
BTB 07807	−1.319	−2.67	Compound12503	−0.754	−3.388
BTB 08814	−0.753	−3.661	Compound13574	−1.4	−2.288
BTB 13767	−0.705	−3.428	Compound15649	−0.746	−2.714
BTB 14330	−0.943	−3.38	Compound19817	−1.127	−2.824
DSH 00533	−0.774	−3.645	Compound20342	−0.6	−3.225
HTS 01124	−0.764	−3.434	Compound20351	−0.76	−2.669
HTS 02708	−0.883	−3.292	Compound20354	−0.996	−2.466
HTS 05096	−0.759	−3.882	Compound20887	−1.055	−3.358
HTS 10008	−0.905	−3.635	Compound21245	−0.538	−3.478
HTS 12786	−1.066	−3.439	Compound23403	−0.974	−3.801
JFD 03179	−0.693	−3.872	Compound25039	−0.941	−3.474
KM 01884	−1.001	−3.112	Compound26856	−0.702	−3.27
NRB 02089	−0.949	−2.177	Compound30002	−0.641	−2.876
NRB 02765	−1.114	−2.387	Compound31095	−1.058	−2.498
RDR 03170	−1.247	−2.813	Compound32927	−0.574	−2.812
SCR 00085	−0.721	−3.861	Compound8921	−1.041	−2.81
–	–	–	Compound8964	−0.953	−3.496
–	–	–	Compound9112	−1.185	−2.7

out the retrieved hit molecules from the databases. Totally, 8 hit molecules from Maybridge and Chembridge databases were selected as potent inhibitors based on the fitness score cut off value of 25. These selected inhibitors were further validated by using the visualization method to find the suitable binding mode of the inhibitors based on the critical interactions with the active site residues. Four and three compounds from Maybridge and Chembridge have shown bifurcate interactions with Asp93 and Thr184. Totally, 7 molecules were selected as good compounds based on GOLD program.

Comparing the results of *LigandFit* and GOLD docking, 3 compounds from Maybridge and 1 compound from Chembridge databases were selected as potent inhibitors of HSP90 which showed a hydrogen bond interactions with the important amino acids like Asp93 and Tyr184 as well as all the molecules have good score (Jain score/*LigandFit* and gold fitness score/GOLD) values (Fig. 8). The HBA of candidate compounds have shown an interaction with Asp93 and the HBD of candidate compounds to interact with CO of Asp93. In addition, the compound bound in the predicted orientation and satisfied the expected hydrophobic interaction as defined by our query (Hypothesis). Furthermore, the candidate compounds satisfied the demands of a chemical features-based and structure-based hypothesis models. From the above results, it has been proved that the screened molecules can effectively disrupt the binding of ATPase and match the structural requirement of a new type of HSP90 inhibitors. Hence, finally, 4 molecules from the databases were selected as most potent inhibitors for HSP90.

2.7. Similarity analysis

The PubChem [33] and Scifinder scholar [34] search tools are used to confirm the novelty of the hit compounds. SID 4259781 and SID 859899 compounds show a partial similarity with our hit compounds. The partial similarity compounds from PubChem databases were tested with the SB_Hypo1, Hypo1 as well as molecular docking studies. In SB_Hypo1, SID 4259781 shows a fit value of 0.9 and SID 859899 fails to screen. In case of Hypo1 both the compounds are not able to fit the geometric constrains. Overall both the compounds form the PubChem database is not able to fit with our best hypotheses. Hence to confirm the orientation of these molecules in the ATP binding site of HSP90, *LigandFit* and GOLD molecular docking was performed. The dock score and Jain score for the hit molecules are far better when compared with the PubChem molecules. The dock score for SID 4259781 and SID 859899 compounds was less than 85 but the database hit molecules shows a value greater than 90. To check the hydrophobic nature of the molecules Jain scoring was calculated, the hit molecules shows a value greater than 4.5 but the PubChem molecules shows a value less than 3.5. Gold fitness score value for these two compounds are less than 25 which were inactive in our case (Table 6). Molecular docking studies also prove that these compounds are not suitable to form hydrogen bond interactions with the critical residues like Asp93 and Thr184. The novelties of the four hit compounds were further confirmed by the Scifinder scholar search tool. Hence we suggest that these four compounds are novel scaffold to inhibit the HSP90 activity.

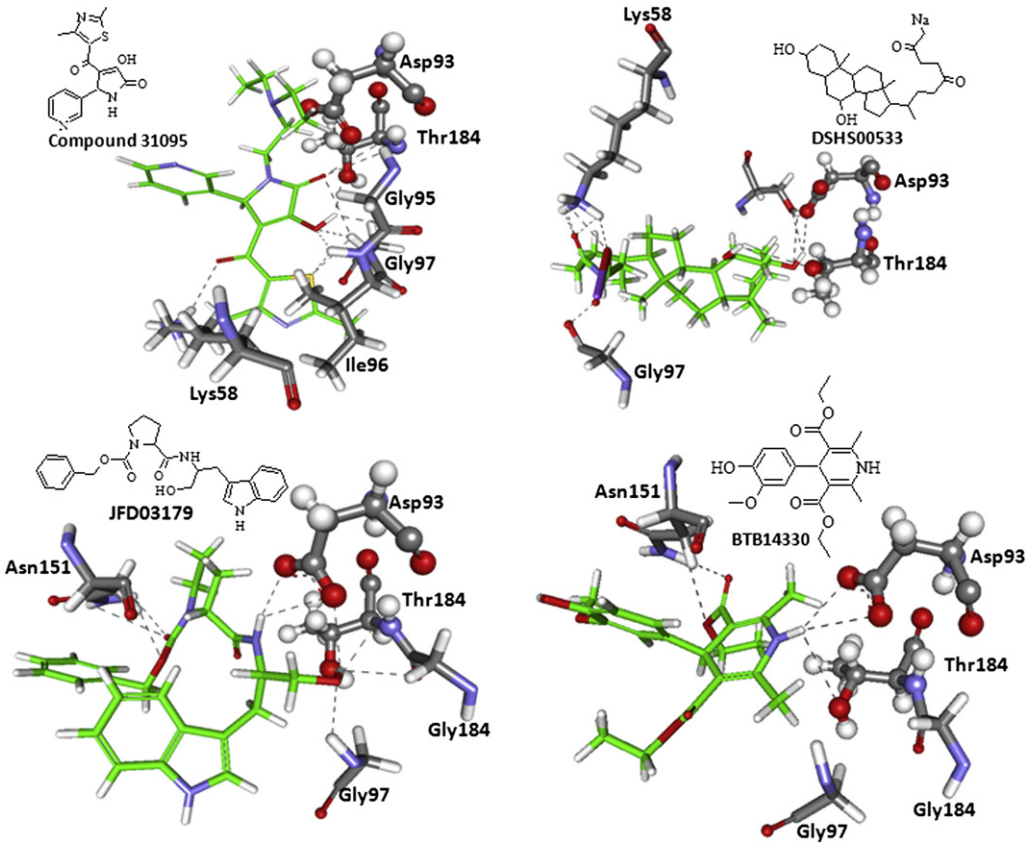

Fig. 8. Hit compounds from Maybridge (DSHS00533, JFD 03179, BTB14330) and Chembridge (Compound 31095) in the active site of heat shock protein 90. Dotted line represents the hydrogen bonds. Ligands are in green color and the critical amino acids Asp93 and Thr184 was represent in ball and stick (for interpretation of the references to colour in this figure legend, the reader is referred to the web version of this article.)

Table 6
Similarity search validation.

Name	Fit value		Jain Score	Dock Score	Gold Fitness Score
	Hypo1	SB_Hypo1			
Compound 31095	2.49	2.61	4.93	93	53
DSHS 00533	4.66	3.56	5.81	91	58
JFD 03179	3.71	4.23	4.66	105	57
BTB 14330	4.06	3.59	4.46	99	56
SID 4259781	–	0.9	3.38	84	22
SID 8595899	–	–	3.42	83	17

3. Conclusions

Inhibition of HSP90 has emerged as a new promising target in the field of antitumor therapy since it influences many signaling pathways. Several structurally diverse compounds possessing growth inhibitory potency against HSP90 over expressing cancer cells were identified using pharmacophore, virtual screening and molecular docking studies. In this study, software packages DS and *LigandScout* were used for the identification and visualization of protein–ligand interaction sites, pharmacophore model generation and database screening. The qualitative pharmacophore model (Hip-Hop) was compare with the structure-based hypothesis to elucidating the critical chemical features to inhibit the activity of HSP90. The qualitative best hypothesis, Hypo1, contains 2 HBA, 1 HBD and 2 H features have been selected based on the cluster analysis, geometrical parameters of the hypothesis as well as validated using test and decoy sets. For structure-based pharmacophore, five different hypotheses were generated based on the HSP90 crystal structures bound with five different ligands. These five hypotheses were superimposed and removed the overlaid features. Finally, the dynamics structure-based hypothesis consist of 8 chemical features which was split into two pharmacophore models: SB_Hypo1 consists of 1 HBA, 1 HBD and 4H groups and SB_Hypo2, 3 HBA, 1 HBD and 2 H chemical groups. These two hypotheses have been validated using test set, SB_Hypo1, selected as a best hypothesis based on its ability in retrieving the active molecules and confirmed by the decoy set which showed good predictive power. Hence, the best hypothesis Hypo1 and the SB_Hypo1 were used as a 3D structural query to screen the chemical databases like as Maybridge and Chembridge for retrieving new potent inhibitors of HSP90. A total of 17 and 19 compounds from Maybridge and Chembridge were selected as common hit molecules from the virtual screening process using Hypo1 and SB_Hypo1 as well as these molecules satisfied the drug like properties, respectively. Hence, the selected molecules were subjected to two molecular docking methods: *LigandFit*/DS and GOLD were applied to select the potent inhibitors of HSP90. *LigandFit*/DS picked 3 and 1 molecules from Maybridge and Chembridge databases applying consensus scoring functions and also the selected molecules were visualized to find the hydrogen bonds with Asp93 and Thr184. From GOLD docking, 4 and 3 molecules from Maybridge and Chembridge were selected based on the gold fitness score as well as the critical hydrogen bonds with Asp93 and Tyr184. By comparing the both docking results, finally, 3 and 1 compounds from Maybridge and Chembridge databases were selected as potent inhibitors of HSP90 which showed good score values and necessary hydrogen bond interactions with both the critical amino acids Asp93 and Tyr184. All these molecules show good interactions. In conclusion, it has shown that, modification of typical pharmacophore and combination of docking with pharmacophore based virtual screening can improve the activity of leads. These hits are under optimization for further drug development to get more druggable lead.

4. Methods and materials

4.1. Pharmacophore modeling

The ligand based and structure-based pharmacophore modeling studies were carried out using the Hip-Hop/DS and *LigandScout*, respectively. Hip-Hop mainly focused on the critical common features present in the set of inhibitors and *LigandScout* generate the structure-based pharmacophore model based on the critical interactions between the protein–ligand.

Ligand and structure-based pharmacophore modeling is the productive tool to discover the compounds with improved potency and pharmacokinetic properties. Ligand based pharmacophore was classified into two categories, first, based on the common features present in the set of molecules and second, is purely based on activity values and the structure of ligands which were present in training set to generate a pharmacophore models. Structure-based pharmacophore model will utilize the interactions between receptor–ligand complexes to generate a hypothesis. The structure-based method becomes increasingly important because the deposit of X-ray crystal structures in PDB was growing rapidly. It was suggested that the information about the protein structure is a good source to bring forth the structure-based pharmacophore and used as first-screening before docking studies [35,36].

4.2. Ligand based approach using DS

The significance of pharmacophore models purely depends on the quality of the molecules used in pharmacophore generation. So the main attention was given to the training set molecule selection, in this work five different HSP90 co-crystal structures were selected from PDB. These five inhibitors, PDB ID: 3BM9, 3HHU, pdb:3BMY, 3FT8, and 3EKR were selected based on the size and activity values (IC_{50}) of the ligands. All the five inhibitors were extracted from its bound structure and the CHARMm force field was applied to verify the bond orders. The 'principal' and 'Max-OmitFeat' values were set to 2 and 0 for all compounds in the training set. HBA, HBD and H features were considered as important chemical features of HSP90 inhibitors based on the published result of HSP90 HypoGen model [3]. Ten hypotheses were generated and the best hypothesis was selected based on the *cluster analysis* module as well as the ranking score of the hypothesis.

4.3. Generation of receptor/structure-based pharmacophore models using LigandScout

Five X-ray co-crystal structures of HSP90 (PDB ID: 3BM9, 3FT8, 3HHU, 3EKR, 3BMY) were used to generate the structure-based pharmacophore models. These five structures were selected based on the resolution and its deposited date.

4.3.1. Structure-based pharmacophore modeling

The ligand interactions with critical amino acids present in the active site of protein was a sufficient input to generate the structure-based pharmacophore. Two software tools were used to key out the crucial pharmacophore patterns: (i) *LigandScout*, used to study the interactions between the inhibitors and amino acids in the active site of HSP90, also used as a tool for automatic construction and visualization of pharmacophore model derived from the 3D coordinates of the proteins [31,37]. The software extracts and interprets ligand–receptor interactions such as hydrogen bond, charge transfer, hydrophobic regions of their macromolecular environment from PDB files. Multiple chemical features were detected and mapped onto the ligand functional groups that are allowing the user to export knowledge on HSP90

inhibitors. Alternative HBA and/or HBD site are considered simultaneously on the protein within the limits of geometric constraints. Excluded volume spheres were also added to the structure-based model onto coordinates defined by protein side chain atoms to characterize the inaccessible areas for any potential ligand (ii) DS was used for the conversion of .hypoedit to .chm file, which is a suitable format for screening the multi-conformational three-dimensional chemical structure databases. The 3D coordination of the interaction point was obtained from *LigandScout* pharmacophore definitions and results in specific interaction model that are able to map the ligands in their bioactive conformation.

4.3.2. Pharmacophore model generation using LigandScout

The *LigandScout* [37] software was used to observe and detect the crucial interactions between the critical amino acids present in the active site of HSP90 and its inhibitors. Stepwise interpretation of the functional group patterns have performed for ligands: planar ring detection, assignment of functional group patterns, determination of the hybridization state and finally the assignment of Kekule pattern. We built the pharmacophore models for HSP90 complexes with five different inhibitors. All the generated hypotheses in .hypoedit format which were translated into .chm using DS/*Hypoedit* scriptto use as 3D query for the virtual screening process.

4.4. Pharmacophore selectivity and evaluation

To validate the generated qualitative and structure-based hypotheses, two kinds of dataset were constructed, test and decoy sets. Test set contains 30 diverse compounds with the activity value (IC_{50}) between 6 nM–200,000 nM, which were classified into active ($IC_{50} < 300$ nM = +++), moderate active (300 nM $\leq$ $IC_{50} < 3000$ nM = ++) and low active ($IC_{50} \geq 3000$ nM = +) HSP90 inhibitors [3]. MDL-ISIS Draw v2.5 was used to sketch the two-dimensional chemical structures of all compounds and converted into their corresponding 3D format by exported into DS. *Best Conformation* module was used to generate the 255 conformations of each compound to assure the energy minimized conformation by applying CHARMm force field and Poling algorithm [38]. The conformations with energy value higher than 20 kcal/mol from the global minimum were rejected. Test set is mainly used to evaluate, how well the selected hypothesis distinguished between active and inactive inhibitors.

Decoy set, was prepared by calculating the 1D property of 1200 molecules The main purpose of this validation is to check how well the generated hypothesis differentiates the active from inactive molecules. Twenty-five active HSP90 antagonists also included in the decoy set to calculate the statistical parameters for the selected best hypothesis such as goodness of hit score (GH), enrichment factor (EF). GH and EF are the two main factors which can predict the capability of the hypothesis.

4.5. In silico screening

Virtual screening was one of the fast and accurate technique to obtain the new leads with desired activity profiles [3]. The representative pharmacophore can be used as a search query for the virtual screening of the multi-conformational databases by applying two distinct algorithms, so-called *FAST* and *BEST Flexible search*, to retrieve the compounds with novel scaffolds and with desired chemical features. Here, *Fast Flexible search* method was used to screen the small molecule databases like Maybridge and Chembridge. It handles the conformational flexibility by pre-generating a representative set of diverse and low energy conformations with the poling algorithm. *Maximum Omitted Features* option was chosen as '0' for the ligand-based pharmacophore models (Hypo1) which was changed into '1' for structure-based pharmacophore (SB_Hypo1) because mapping all features present in the structure-based hypothesis will reduce the hit rate. The resulting hit molecules were ranked according to their geometric fit value that indicates how well the molecules were mapped onto the hypothesis features location constraints and their distance deviation from the feature centers. The compounds with highest fit values were extracted and subjected to ADME and Lipinski's rule of five to refine the hit molecules. Test set molecules and the hit leads which satisfied the chemical features present in both the hypotheses were selected as an input for molecular docking using *LigandFit*/DS and GOLD programs.

4.6. Molecular docking protocols

Combining the virtual screening and molecular docking techniques have become one of the reputable methods in drug discovery and enhancing the efficiency in lead optimization. To evaluate the accuracy of docking, two docking software's were used in this study for the purpose of getting unbiased results of docking, *LigandFit*/DS and GOLD.

Most of the docking algorithms assume the protein as a rigid object which leads to poor correlation of docking scores with the experimental binding affinities of ligands [39,40]. There is no single docking algorithm or scoring function that can correctly predict the binding affinities of ligands in every protein–ligand complex [39,40]. Hence in this study two different docking programs (*LigandFit* and GOLD) were investigated on the test set molecules as well as the leads to identify the binding mode of ligands in the active pocket of a protein and to predict the binding affinity between the ligand and the protein [20].

4.6.1. LigandFit/DS docking

LigandFit was executed for accurate orientation of the ligands into the protein active site. For docking study, protein was prepared by removing all the water molecules and CHARMm force field was applied. The active site was identified by the volume occupied by co-crystal and the critical residues were selected by examining the 40 HSP90 co-crystal structures from PDB. Throughout the docking process top ten conformations were generated for each ligand after the energy minimization using the smart minimize method, which begins with steepest descent method and followed by the conjugate gradient method. Each of the saved conformation was evaluated and ranked using the scoring functions including LigScore1, LigScore2, PLP1, PLP2, JAIN, PMF and LUDI. In this work, Jain score was used to select the leads which were further evaluated by visual inspection of protein–ligand interactions. All the ligands, which formed the good hydrophobic and hydrogen bond interactions with Asn51, Ala55, Lys58, Gly97, Met98, Phe138 and Asp93, Thr184, respectively, were selected as the potent leads for HSP90.

4.6.2. GOLD docking

GOLD v4.1 (http://gold.ccdc.cam.ac.uk./index.php) was used for predict, how well the flexible molecules bind into the proteins active site. This program is using a genetic algorithm methodology for protein–ligand docking that allows full ligand and partial protein flexibility. Crystal structure of HSP90 was selected from PDB for docking process, hydrogen atoms were added, and all water molecules were removed from the protein. To simplify the docking calculations, the binding site of the ligand was defined as a 8 Å radius from the bound ligand and used as an input for GOLD calculations. Docking calculations were performed using the default GOLD fitness function and default evolutionary parameters: population size = 100; selection pressure = 1.1; # operations = 100,000;

islands = 5; niche size = 2; migration = 10; mutation = 95; crossover = 95. Ten docking runs were performed per structure unless three of the 10 poses were within 1.5 Å RMSD of each other. All the hit molecules as well as test set compounds were docked into ATP binding site of HSP90. The interacting ability of a compound depends on the fitness score, greater the GOLD fitness score better the binding affinity. Hit molecules which showed the expected interactions with the critical amino acids present in the active site of the protein, and comparable high binding scores with the bound ligand, were selected as potent inhibitors of HSP90. Finally, combining the results from *LigandFit* and GOLD, the potent HSP90 inhibitors were keyed out.

4.7. Similarity analysis

The similarity analysis was carried out for the four hit compounds using PUBMED search. Compound 310095 shows partial similarities with the PubChem Databases compounds (SID 4259781 and 859899) which were reported as an inactive against HSP90. Hence we carried out a screening process using the best pharmacophore models such as Hypo1 and SB_Hypo1 as well the molecular docking studies (LigandFit and GOLD) using the same parameters which was used to select the hit molecules from the databases.

Acknowledgement

All students were supported by Basic Science Research Program (2009-0073267), Pioneer Research Center Program (2009-0081539) through the National Research Foundation of Korea (NRF) funded by the Ministry of Education, Science and Technology (MEST). Fundamental Technology Development Program (2010-0029084).

References

[1] W. Paul, Cancer Detect. Prev. 26 (2002) 405–410.
[2] M. Sgobba, G. Rastelli, Chem. Med. Chem. 4 (2009) 1399–1409.
[3] S. Sakkiah, S. Thangapandian, S. John, Y.J. Kwon, K.W. Lee, Eur. J. Med. Chem. 45 (2010) 2132–2140.
[4] C. Yin, C. Ellen, Henry, A. Thomas, Biochemistry 48 (2009) 180–189.
[5] R. Bagatell, L. Whitesell, Mol. Cancer Ther. 3 (2004) 1021–1030.
[6] K. Terasawa, M. Minami, Y. Minami, J. Biochem. 137 (2005) 443–447.
[7] X.Q. Deng, H.Y. Wang, Y.L. Zhao, M.L. Xiang, P.D. Jiang, Z.X. Cao, Y.Z. Zheng, S.D. Luo, L.T. Yu, Y.Q. Wei, S.Y. Yang, Chem. Biol. Drug Des. 71 (2008) 533–539.
[8] D.B. Solit, G. Chiosis, Drug Discov. Today 13 (2008) 38–43.
[9] M.C. Rosenhagen, C. Sti, U. Schmidt, G.M. Wochnik, F.U. Hartl, F. Holsboer, J.C. Young, T. Rein, Mol. Endocrinol. 17 (2003) 1991–2001.
[10] G. Chiosis, M. Vilenchik, J. Kim, D. Solit, Drug Discov. Today 9 (2004) 881–888.
[11] A.S. Sreedhar, E. Kalmar, P. Csermely, Y.F. Shen, FEBS. Lett. 563 (2004) 11–15.
[12] S. Ramadevi, T. Sunita, G. Rambabu, S. Vadivelan, P.K. Machiraju, R. Dayam, L. Narasu, S. Jagarlapudi, N. Neamati, J. Mol. Grap. Model. 28 (2009) 472–477.
[13] M.J. Egorin, D.M. Rosen, J.H. Wolff, P.S. Callery, S.M. Musser, J.L. Eiseman, Cancer Res. 58 (1998) 2385–2396.
[14] X. Barril, P. Brough, M. Drysdale, R.E. Hubbard, A. Massey, A. Surgenor, L. Wright, Bioorg. Med. Chem. Lett. 15 (2005) 5187–5191.
[15] Y. Li, T. Zhang, S.J. Schwartz, S. Sun, Drug Resist. Update 12 (2009) 17–27.
[16] H. Zhang, F. Burrows, J. Mol., M.G. Klebe, Drug Discov. Today 11 (2006) 580–594.
[17] I. Muegge, S. Oloff, Drug Discov. Today Technol. 3 (2006) 405–411.
[18] C.A. Dickey, J. Eriksen, A. Kamal, F. Burrows, S. Kasibhatala, C.B. Eckman, M. Hutton, L. Petrucelli, Curr. Alzheimer Res. 2 (2005) 231–238.
[19] M.W. Amolins, B.S. Blagg, J. Mini. Rev. Med. Chem. 9 (2009) 140–152.
[20] G. Klebe, Drug Discov. Today 11 (2006) 580–594.
[21] H.D. Holtje, W. Sippl, D. Rognan, G. Folkers, Molecular Modeling Basic Principles Nad Applications, third ed.. Wiley-VCH, Weinheim, 2003.
[22] Maybridge Chemical Company Ltd, Maybridge Chemical Database; Trevillet, Tintangel, Cornwall PL340HW, England, http://www.maybridge.com
[23] http://www.chembridge.com.
[24] C.M. Venkatachalam, X. Jiang, T. Oldfield, M. Waldman, J. Mol. Grap. Model. 21 (2003) 289–307.
[25] G. Jones, P. Willet, R.C. Glen, J. Mol. Biol. 245 (1995) 43–53.
[26] A.C. Wallace, R.A. Laskowski, J.M. Thornton, Protein Eng. 8 (1996) 127–134.
[27] A. Gopalsamy, M. Shi, J. Golas, E. Vogan, J. Jacob, M. Johnson, F. Lee, R. Nilakantan, R. Petersen, K. Svenson, R. Chopra, M.S. Tam, Y. Wen, J. Ellingboe, K. Arndt, F. Boschelli, J. Med. Chem. 51 (2008) 373–375.
[28] R.I. Feldman, B. Mintzer, D. Zhu, J.M. Wu, S.L. Biroc, S. Yuan, K. Emayan, Z. Chang, D. Chen, D.O. Arnaiz, J. Bryant, X.S. Ge, M. Whitlow, M. Adler, M.A. Polokoff, W. Li, M. Ferrer, T. Sato, J.M. Gu, J. Shen, J.L. Tseng, H. Dinter, B. Buckman, Chem. Biol. Drug Des. 74 (2009) 43–50.
[29] J.J. Barker, O. Barker, R. Boggio, V. Chauhan, R.K.Y. Cheng, V. Corden, S.M. Courtney, N. Edwards, V.M. Falque, F. Fusar, M. Gardiner, M. Estelle, N. Hamelin, T. Hesterkamp, O. Ichihara, R.S. Jones, O. Mather, C.S. Minucci, C.A.G.N. Montalbetti, D. Patel, B.G. Phillips, M. Varasi, M. Whittaker, D. Winkler, C. Yarnold, Chem. Med. Chem. 4 (2009) 963–966.
[30] P.P. Kung, F. Lee, M. Jerry, C. Michael, Z.Z. Joe, M.C. Johnson, E. Anne, W. Jeff, M. Pramod, Y. Min-Jean, R. Caroline, F.D. Jay, B. Eileen, S. Tod, A.M. Karen, R.G. Michael, Bio. Med. Chem. Lett. 18 (2008) 6273–6278.
[31] G. Wolber, T. Langer, J. Chem. Info. Comput. Sci. 45 (2005) 160–169.
[32] G. Jones, P. Willet, R.C. Taylor, J. Mol. Biol. 267 (1995) 727–748.
[33] Y. Wang, E. Bolton, S. Dracheva, K. Karapetyan, B.A. Shoemaker, T.O. Suzek, J. Wang, J. Xiao, J. Zhang, S.H. Bryant, Nucl. Acids Res. 38 (2010) D255–D266.
[34] A.B. Wagner, SciFinder scholar 2006, J. Chem. Inf. Model. 46 (2006) 767–774.
[35] D. Joseph, J.C. Alvarez, Proteins 51 (2003) 189–202.
[36] M.L. Barreca, L. De Luca, L. Iraci, A. Rao, S. Ferro, G. Maga, A. Chimirri, J. Chem. Inf. Model. 47 (2007) 557–562.
[37] LigandScout, Version 1.0; Inte:Ligand GmbH, Clemesn-Maria-Hofbaurer-G. 6, 2344, Maria Enzersdorf, Austria. HYPERLINK "http://www.inteligand.com.
[38] A. Smellie, S.L. Teig, P.J. Towbin, Comput. Chem. 16 (1995) 171–187.
[39] R.A. Friesner, J.L. Banks, R.B. Murphy, T.A. Halgren, J.J. Klicic, D.T. Mainz, M.P. Repasky, E.H. Knoll, M. Shelley, J.K. Perry, D.E. Shaw, P. Francis, P.S. Shenkin, J. Med. Chem. 47 (2004) 1739–1749.
[40] T.A. Halgren, R.B. Murphy, R.A. Friesner, H.S. Beard, L.L. Frye, W.T. Pollard, J.L. Banks, J. Med. Chem. 47 (2004) 1750–1759.
[41] P.A. Brough, X. Barril, M. Beswick, B.W. Dymock, M.J. Drysdale, L. Wright, K. Grant, A. Massey, A. Surgenor, P. Workman, Bioorg. Med. Chem. Lett. 15 (2005) 5197–5201.
[42] P.A. Brough, W. Aherne, X. Barril, J. Borgognoni, K. Boxall, J.E. Cansfield, K.M. Cheung, I. Collins, N.G.M. Davies, M.J. Drysdale, B. Dymock, S.A. Eccles, H. Finch, A. Fink, A. Hayes, R. Howes, R.E. Hubbard, K. James, A.M. Jordan, A. Lockie, V. Martins, A. Massey, T.P. Matthews, E. Mcdonald, C.J. Northfield, L.H. Pearl, C. Prodromou, S. Ray, F.I. Raynaud, S.D. Roughley, S.Y. Sharp, A. Surgenor, D.L. Walmsley, P. Webb, M. Wood, P. Workman, L. Wright, J. Med. Chem. 51 (2008) 196–218.
[43] T.E. Barta, J.M. Veal, J.W. Rice, J.M. Partridge, R.P. Fadden, W. Ma, M. Jenks, L. Geng, G.J. Hanson, K.H. Huang, A.F. Barabasz, B.E. Foley, J. Otto, S.E. Hall, Bioorg. Med. Chem. Lett. 18 (2008) 3517–3521.
[44] A. Kreusch, S. Han, A. Brinker, V. Zhou, H.S. Choi, Y. He, S.A. Lesley, J. Caldwell, X.J. Gu, Biorg. Med. Chem. Lett. 15 (2005) 1475–1478.
[45] C.E. Stebbins, A.A. Russo, C. Schneider, N. Rosen, F.U. Hartl, N.P. Pavletich, Cell 89 (1997) 239–250.
[46] J.R. Huth, C. Park, A.M. Petros, A.R. Kunzer, M.D. Wendt, X. Wang, C.L. Lynch, J.C. Mack, K.M. Swift, R.A. Judge, J. Chen, P.L. Richardson, S. Jin, S.K. Tahir, E.D. Matayoshi, S.A. Dorwin, U.S. Ladror, J.M. Severin, K.A. Walter, D.M. Bartley, S.W. Fesik, S.W. Elmore, P.J. Hajduk, Chem. Boil. Drug Des. 70 (2007) 1–12.
[47] J.M. Jez, J.C. Chen, G. Rastelli, R.M. Stroud, D.V. Santi, Chem. Biol. 10 (2003) 361–368.
[48] R. Howes, X. Barril, B.W. Dymock, K. Grant, C.J. Northfield, A.G. Robertson, A. Surgenor, J. Wayne, L. Wright, K. James, T. Matthews, K.M. Cheung, E. Mcdonald, P. Workman, M.J. Drysdale, Anal. Biochem. 350 (2006) 202–213.
[49] X. Barril, M.C. Beswick, A. Collier, M.J. Drysdale, B.W. Dymock, A. Fink, K. Grant, R. Howes, A.M. Jordan, A. Massey, A. Surgenor, J. Wayne, P. Workman, L. Wright, Bioorg. Med. Chem. Lett. 16 (2006) 2543–2548.
[50] L. Wright, X. Barril, B. Dymock, L. Sheridan, A. Surgenor, M. Beswick, M. Drysdale, A. Collier, A. Massey, N. Davies, A. Fink, C. Fromont, W. Aherne, K. Boxall, S. Sharp, P. Workman, R.E. Hubbard, Chem. Biol. 11 (2004) 775–785.
[51] S.Y. Sharp, C. Prodromou, K. Boxall, M.V. Powers, J.L. Holmes, G. Box, T.P. Matthews, K.M. Cheung, A. Kalusa, K. James, A. Hayes, A. Hardcastle, B. Dymock, P.A. Brough, X. Barril, J.E. Cansfield, L.M. Wright, A. Surgenor, N. Foloppe, R.E. Hubbard, W. Aherne, L. Pearl, K. Jones, E. Mcdonald, F. Raynaud, S. Eccles, M. Drysdale, P. Workman, Mol. Cancer Ther. 6 (2007) 1198–1211.
[52] B.W. Dymock, X. Barril, P.A. Brough, J.E. Cansfield, A. Massey, E. Mcdonald, R.E. Hubbard, A. Surgenor, S.D. Roughley, P. Webb, P. Workman, L. Wright, M.J. Drysdale, J. Med. Chem. 48 (2005) 4212–4215.
[53] R.M. Immormino, Y. Kang, G. Chiosis, D.T. Gewirth, J. Med. Chem. 49 (2006) 4953–4960.
[54] M. Congreve, G. Chessari, D. Tisi, A.J. Woodhead, J. Med. Chem. 51 (2008) 3661–3680.
[55] P.P. Kungg, L. Funk, J. Meng, M. Collins, J.Z. Zhou, M.C. Johnson, A. Ekker, J. Wang, P. Mehta, M.J. Yin, R.C. Odgers, J.F. Davies, E. Bayman, T. Smeal, K.A. Maegley, M.R. Gehring, Bioorg. Med. Chem. Lett. 18 (2008) 6273–6278.